

# ATP-Uncoupled, Six-Electron Photoreduction of Hydrogen Cyanide to Methane by the Molybdenum–Iron Protein

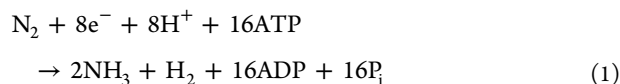
Lauren E. Roth and F. Akif Tezcan\*

Department of Chemistry and Biochemistry, University of California, San Diego, La Jolla, California 92093-0356, United States

**S** Supporting Information

**ABSTRACT:** A detailed study of the eight-electron/eight-proton catalytic reaction of nitrogenase has been hampered by the fact that electron and proton flow in this system is controlled by ATP-dependent protein–protein interactions. Recent studies have shown that it is possible to circumvent the dependence on ATP through the use of potent small-molecule reductants or light-driven electron injection, but success has been limited to two-electron reductions of hydrazine, acetylene, or protons. Here we show that a variant of the molybdenum–iron protein labeled with a Ru-photosensitizer can support the light-driven, six-electron catalytic reduction of hydrogen cyanide into methane and likely also ammonia. Our findings suggest that the efficiency of this light-driven system is limited by the initial one- or two-electron reduction of the catalytic cofactor (FeMoco) to enable substrate binding, but the subsequent electron-transfer steps into the FeMoco-bound substrate proceed efficiently.

The inertness of N<sub>2</sub> translates into a high energetic cost for its reduction into NH<sub>3</sub>.<sup>1</sup> In the industrial Haber–Bosch process for nitrogen fixation, this cost is expressed in the form of high temperatures and high pressures of H<sub>2</sub> and N<sub>2</sub>.<sup>2</sup> While the biological reduction of N<sub>2</sub> catalyzed by nitrogenase proceeds at room temperature and atmospheric pressure, it still requires the hydrolysis of a staggering number of ATP molecules for every turnover reaction:<sup>2,3</sup>



In this reaction, the electron transfer (ET) steps are coupled to ATP hydrolysis by the iron–protein (FeP) component of nitrogenase. FeP delivers one electron at a time to the catalytic iron–molybdenum protein (MoFeP) while hydrolyzing two ATP molecules. N<sub>2</sub> reduction by the active site cofactor of MoFeP, the so-called FeMoco, strictly requires FeP as an external reductant under constant ATP turnover.<sup>2</sup> Because these conditions produce continuous electron flow into MoFeP, it has been challenging to populate and maintain discrete catalytic intermediates bound to FeMoco for thorough structural characterization.<sup>4,5</sup> The complex, ATP-dependent interactions between FeP and MoFeP have further complicated the understanding of internal ET steps within MoFeP.<sup>6</sup> In addition, because the rate-limiting step in the overall N<sub>2</sub> reduction reaction is the dissociation of the ADP-bound FeP

from MoFeP,<sup>7</sup> many critical ET and proton transfer (PT) steps within MoFeP are likely to be masked when nitrogenase catalysis is studied under ATP turnover. Clearly, new experimental strategies are needed to uncouple biological N<sub>2</sub> fixation from ATP hydrolysis and FeP-mediated ET, which in turn would pave the way to in-depth studies of the complex ET, PT, and substrate activation steps within MoFeP.

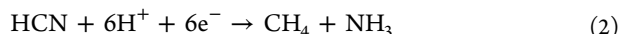
Along these lines, it was recently reported that a MoFeP variant ( $\beta$ -Y98H) could be driven by the strong, electrochemically generated reductants Eu<sup>II</sup>-EGTA and Eu<sup>II</sup>-DTPA to catalyze the two-electron reduction of N<sub>2</sub>H<sub>4</sub> to NH<sub>3</sub> in the absence of FeP and ATP.<sup>8</sup> At the same time, we reported that a MoFeP variant ( $\alpha$ -L158C) labeled on its surface with a Ru-polypyridine photosensitizer could be photoactivated to catalyze the two-electron reductions of H<sup>+</sup> and C<sub>2</sub>H<sub>2</sub> into H<sub>2</sub> and C<sub>2</sub>H<sub>4</sub>, respectively.<sup>9,10</sup> The quantum yield ( $\phi$  = catalytically useful electrons/photons absorbed) of this particular light-driven system is low (ca. 1%). Nevertheless, it offers the important advantage that the reduction of MoFeP is unimolecular and can be initiated rapidly, which is a prerequisite to interrogating the fleeting redox intermediates populated during substrate reduction. Another important milestone toward completely bypassing ATP/FeP-dependence and driving the native eight-electron catalytic reaction (eq 1) with light is the delivery of multiples of two electrons to FeMoco. With that goal in mind, we show here the catalytic reduction of HCN into CH<sub>4</sub> by Ru-labeled MoFeP. To our knowledge, this represents the first light-driven six-electron catalytic reaction by a redox enzyme.<sup>11</sup> Our findings support the presence of an ET-gating process within MoFeP and suggest that once FeMoco attains one- or two-electron-reduced states (E<sub>1</sub> or E<sub>2</sub>), the subsequent reduction of the bound substrates proceeds with high efficiency.

Nitrogenase can catalyze the reduction of numerous multiply bonded molecules besides N<sub>2</sub>, including CO,<sup>12,13</sup> CO<sub>2</sub>,<sup>14</sup> and HCN.<sup>15–17</sup> HCN is a particularly intriguing substrate because it is isoelectronic with N<sub>2</sub> and features a similarly strong (887 kJ/mol) triple bond. HCN is likely reduced and protonated six-fold through a pathway that is similar to that suggested for N<sub>2</sub>.<sup>6,16–18</sup> Furthermore, it was recently shown that the isolated FeMoco can reduce HCN in the presence of Eu<sup>II</sup>-DTPA with nearly the same yield as nitrogenase under ATP turnover conditions.<sup>19</sup> Importantly, while N<sub>2</sub> binding to FeMoco requires the cofactor to be reduced by 3 or 4 electrons (E<sub>3</sub> or E<sub>4</sub>) beyond its resting state under high electron flux,<sup>20</sup> HCN

Received: April 4, 2012

Published: May 7, 2012

or its conjugate base  $\text{CN}^-$  (proposed to be an inhibitor) can bind FeMoco under low electron flux conditions, where they can compete with  $\text{H}^+$  binding and reduction.<sup>16</sup> Indeed, we previously observed that  $\text{HCN}/\text{CN}^-$  effectively suppressed photoinduced  $\text{H}^+$  and  $\text{C}_2\text{H}_2$  reduction by Ru-labeled MoFeP.<sup>9</sup> This observation prompted the possibility that  $\text{HCN}$  may be reduced with our light-activated system to generate  $\text{CH}_4$  or methylamine ( $\text{CH}_3\text{NH}_2$ ):



As a first step toward this end, we prepared the  $\alpha$ -C45A/L158C mutant of *Azotobacter vinelandii* MoFeP (see Supporting Information (SI) and Figure S1 for details on mutagenesis and characterization), which features only a single accessible surface cysteine ( $\alpha$ -C158) for modification with the iodoacetamido derivative of  $[\text{Ru}(\text{bpy})_2(\text{phen})]^{2+}$  (IA-RuBP) (Figure 1a).<sup>21</sup> Quantitative labeling with IA-RuBP was confirmed by

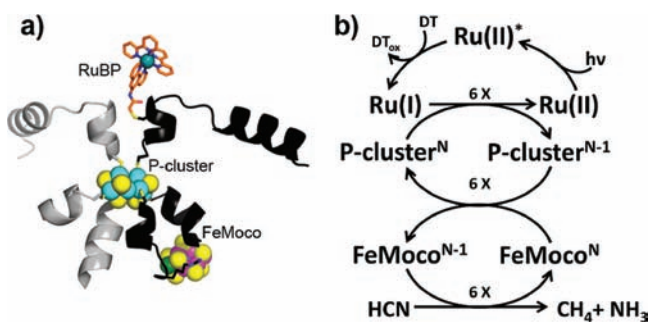


**Figure 1.** (a) Structural model for Ru-MoFeP, in which the Ru-label is covalently attached to residue  $\alpha$ -C158. Approximate edge-to-edge distances are 16 Å (RuBP–P-cluster) and 14 Å (P-cluster–FeMoco).  $\alpha$ -helices anchoring the P-cluster and FeMoco in the  $\alpha$ - and  $\beta$ -subunits of MoFeP are highlighted in black and gray, respectively. (b) Proposed photocatalytic scheme for the six-electron reduction of  $\text{HCN}$  to  $\text{CH}_4$  and  $\text{NH}_3$ . Dithionite (DT) acts as a reductive quencher for the high-yield generation of Ru(I) species.

inductively coupled optical emission spectroscopy (ICP-OES), which indicated the presence of one label per each  $\alpha\beta$ -subunit of MoFeP (Table S1, SI). We will hereafter refer to the labeled protein simply as Ru-MoFeP. SDS-PAGE results showed that labeling on Ru-MoFeP was limited to the  $\alpha$ -subunit as expected (Figure S2, SI). Photoinduced  $\text{H}^+$  reduction assays with Ru-MoFeP showed comparable levels of activity (Figure S3, SI) to the previously tested  $\alpha$ -L158C mutant, which had two RuBP labels per  $\alpha\beta$ -subunit.

A typical reaction solution for photoinduced  $\text{HCN}$  reduction included 2.7 mg of Ru-MoFeP (23 nmol of active sites), 200 mM sodium dithionite ( $\text{Na}_2\text{S}_2\text{O}_4$ ) as the reductive quencher, 10 mM NaCN, 200 mM NaCl, and 100 mM HEPES at pH 6.5–7.5. The proposed photocatalytic scheme is shown in Figure 1b. Reaction solutions were irradiated in a 20 °C water bath with a Xe/Hg lamp using UV- and IR-cutoff filters under constant stirring, and the head gas was analyzed for products by gas chromatography mass spectrometry (GC-MS). Irradiating the reaction solutions that contained all of the above components led to the appearance of a peak that was determined through GC standards and MS to be  $\text{CH}_4$  (Figure 2a). Substitution of NaCN with the isotopically labeled substrate,  $\text{Na}^{13}\text{CN}$ , led to a 1 amu shift in the mass of the

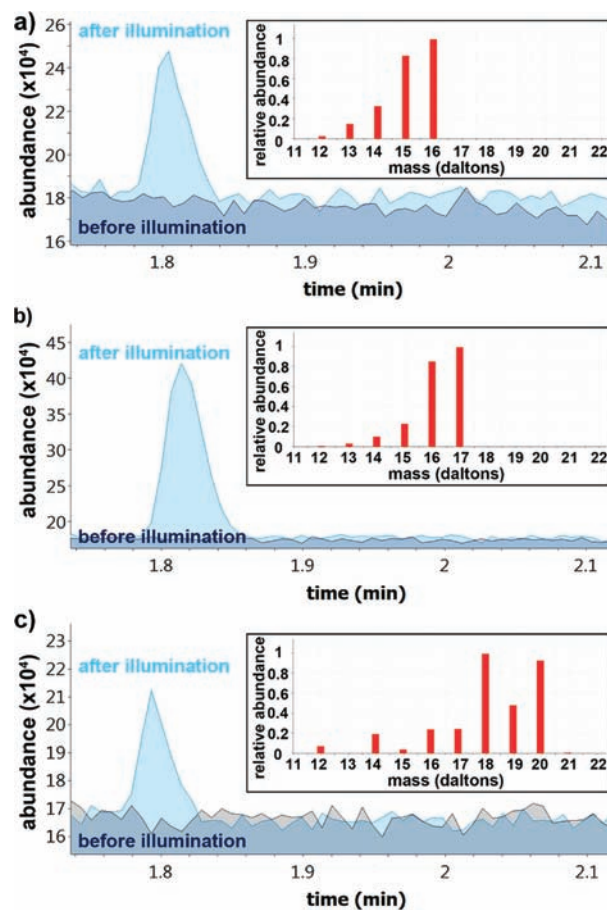


**Figure 2.** GC-MS analysis for  $\text{CH}_4$  production during photoreduction experiments with Ru-MoFeP. The GC traces were acquired before (blue) or after 1 h illumination (cyan) of the samples that contain (a) NaCN, (b)  $\text{Na}^{13}\text{CN}$ , or (c) NaCN dissolved in deuterated buffer solution. In (c), we ascribe the presence of the peaks for partially deuterated products to protons associated with the MoFeP interior that were not completely exchanged into the deuterated buffer solution.

product peak (to 17 amu), confirming that  $\text{CH}_4$  results from the reduction of  $\text{HCN}/\text{CN}^-$  (Figure 2b). Reactions performed in 90%  $\text{D}_2\text{O}$  produced the 20 amu product,  $\text{CD}_4$ , as well as other partially deuterated methane isotopomers, indicating that the hydrogens in the product originated from protons in the bulk solution (Figure 2c). In addition to  $\text{CH}_4$ , nitrogenase catalyzed  $\text{HCN}/\text{CN}^-$  reduction should also produce an equimolar amount of  $\text{NH}_3$  (eq 2) and possibly,  $\text{CH}_3\text{NH}_2$  (eq 3). Yet, the high concentrations of dithionite needed for photocatalytic turnover precluded the quantification of  $\text{NH}_3$  or  $\text{CH}_3\text{NH}_2$ , as dithionite readily reacts with the fluorescent indicators used for the detection of amine-containing species and deactivates them (see Figure S4 and Materials and Methods, SI).

Under constant irradiation at pH 7.0 and 10 mM NaCN, the production of  $\text{CH}_4$  proceeded with an initial velocity (measured between 0 and 15 min) of 0.4 nmol  $\text{CH}_4$ /min per mg of MoFeP. In the absence of any one component from the complete reaction system (light, RuBP, MoFeP, dithionite, NaCN, or covalent attachment of RuBP to MoFeP), no  $\text{CH}_4$  was produced (Figure 3a). As we previously observed with photoinduced  $\text{H}_2$  and  $\text{C}_2\text{H}_4$  formation,<sup>9</sup>  $\text{CH}_4$  production eventually reached a plateau after approximately 90 min

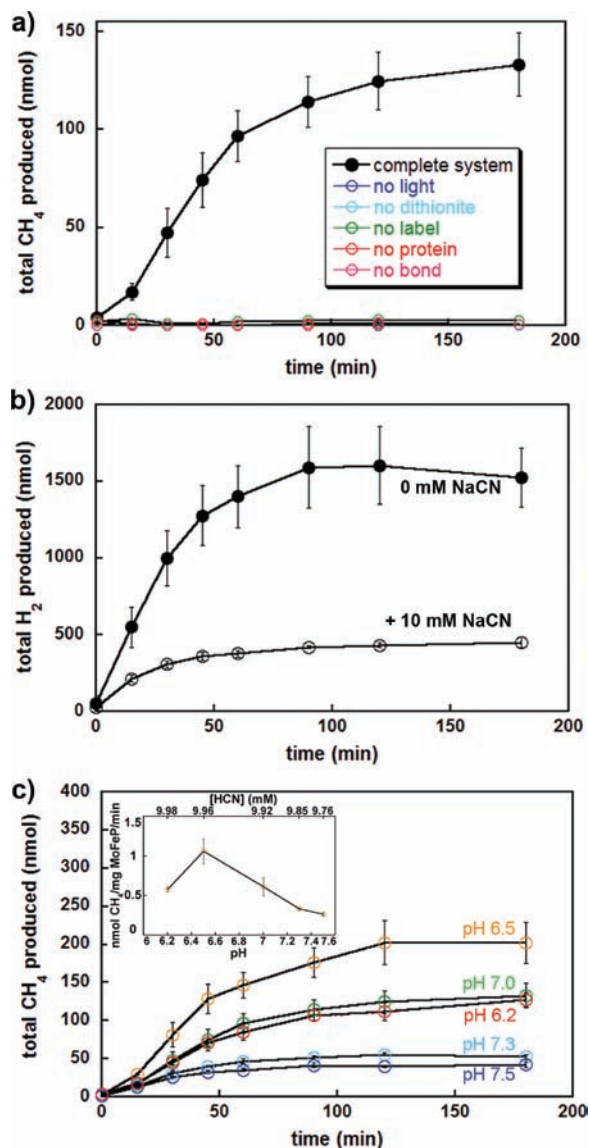


**Figure 3.** (a) Cyanide reduction assays (black) and corresponding controls, each of which is missing the indicated component of the complete reaction system. All measurements were done in triplicate. (b) H<sub>2</sub> production during photoreduction assays in the presence (open circles) or absence (filled circles) of NaCN. (c) Dependence of CH<sub>4</sub> production on pH. (Inset) Changes in the rate of CH<sub>4</sub> formation (based on the first 45 min of irradiation) as a function of pH.

(Figure 3a). This loss in activity appears likewise to be due to ligand substitution on the RuBP functionality, whereby the metal-to-ligand charge transfer (MLCT) bands of RuBP steadily disappear during turnover ( $\tau = 26.4 \pm 0.9$  min, Figure S5, SI), paralleling the tapering of CH<sub>4</sub> production.

In addition to producing 130 nmol CH<sub>4</sub> at pH 7.0 and 10 mM NaCN, the Ru-MoFeP system also generated 450 nmol H<sub>2</sub> from simultaneous H<sup>+</sup> reduction. This translates into a total of 1680 nmol of electrons transferred during catalysis, which likely is an underestimate, as it does not account for partial HCN reduction to either CH<sub>3</sub>NH<sub>2</sub> or a two-electron reduced intermediate that may be hydrolyzed to formaldehyde and NH<sub>3</sub>.<sup>18,22</sup> In comparison, under the same reaction conditions but without NaCN, the system was able to transfer a total of 3200 nmol of electrons when only catalyzing the reduction of H<sup>+</sup> (Figure 3b). Studies have shown that the CN<sup>-</sup> ion is a

strong inhibitor of total electron flow during nitrogenase turnover, which may explain the reduction in the total amount of electrons transferred to substrates (HCN and H<sup>+</sup>).<sup>15,17</sup> The quantum yield for CH<sub>4</sub> formation at pH 7.0 (based on the initial 15 min of activity) is calculated to be ca. 0.07%, compared with 0.86% for H<sub>2</sub> production in the absence of NaCN. If each successive transfer of two electrons from RuBP to FeMoco and the substrates were governed by the same mechanism and proceeded with the same efficiency, the theoretical yield of CH<sub>4</sub> formation would be  $(0.86\%)^3 = 6.3 \times 10^{-7}$ . The fact that the observed yield is more than 1100-fold higher than the theoretical yield indicates that the individual ET steps from RuBP into FeMoco during the six-electron HCN reduction are not equivalent. It is commonly believed that there must be a FeP-induced conformational change within MoFeP, which controls the initial reduction of FeMoco and the subsequent binding of substrates.<sup>4,23</sup> We propose that, in the absence of activation of this gate by ATP-dependent FeP binding, the probability of reaching the E<sub>1</sub> or E<sub>2</sub> states of FeMoco is low, leading to diminished yields of H<sup>+</sup> and HCN binding and reduction relative to the ATP-driven system. Nevertheless, as implied by the disproportionately high yields of CH<sub>4</sub>, once HCN is committed to the catalytic cycle upon reaching the E<sub>1</sub> or E<sub>2</sub> states, the subsequent reduction steps proceed with relatively high efficiency.

The extent of photoinduced CH<sub>4</sub> production by Ru-MoFeP strongly depends on the solution pH (Figure 3c). The maximal activity occurs at ca. pH 6.5 with a quantum yield for CH<sub>4</sub> production ( $\phi \approx 0.13\%$ ) that is nearly twice as much as that at pH 7.0 and 5 times as much as that at pH 7.5. As shown in the inset of Figure 3c, the increase in activity between pH 7.5 and 6.5 does not scale with a decrease in the concentration of the inhibitor, CN<sup>-</sup> ( $pK_a = 9.2$ ). The activity for photoinduced H<sub>2</sub> formation also peaks at pH 6.5 (Figure S6, SI). Burgess and colleagues observed similar, bell-shaped pH vs activity profiles with *A. vinelandii* nitrogenase for various substrates (N<sub>2</sub>, H<sup>+</sup>, C<sub>2</sub>H<sub>2</sub>) under ATP/FeP-dependent turnover conditions.<sup>24</sup> A distinction between the profiles for photoinduced and ATP/FeP-driven reduction processes is that the latter shows maximal activity at a full pH unit higher (ca. pH 7.5) than the former. This shift may well stem from a mechanistic difference between the photoinduced and the ATP/FeP-driven reactions, where the rate-determining steps for substrate reduction may involve different protonatable residues. In the case of the photoinduced reaction, a transition in activity occurs with a midpoint at ca. pH = 7, invoking the participation of a histidine residue. Alternatively, the shift may simply be a manifestation of the fact that the ATP/FeP-driven reaction involves complex, pH-dependent steps upstream from substrate reduction that are bypassed in the photoinduced reaction (e.g., ATP-binding/hydrolysis and FeP-MoFeP interactions).

In summary, we have reported here the light-driven, six-electron reduction of HCN by MoFeP. Our results suggest that the efficiency of our ATP-uncoupled system is primarily limited by the initial reduction of FeMoco, which is believed to be gated by an ATP/FeP-dependent conformational change in the native system. Given the recent evidence that this conformational change may be mimicked by simple amino acid substitutions,<sup>8</sup> it should be possible to drive the full eight-electron catalytic cycle of nitrogenase by light and examine the unexplored details of its mechanism.

## ■ ASSOCIATED CONTENT

### 📄 Supporting Information

Materials/methods, supporting table for ICP-OES measurements, supporting figures for protein characterization and various activity assays. This material is available free of charge via the Internet at <http://pubs.acs.org>.

## ■ AUTHOR INFORMATION

### Corresponding Author

tezcan@ucsd.edu

### Notes

The authors declare no competing financial interest.

## ■ ACKNOWLEDGMENTS

We thank Dr. Robert Pomeroy and Dr. John Limtiaco for assistance with GC-MS measurements. This work was supported by the NSF (predoctoral fellowship to L.E.R., MCB-0643777 to F.A.T.) and ACS (PRF-G 46939-G3).

## ■ REFERENCES

- (1) Galloway, J. N.; Cowling, E. B. *Ambio* **2002**, *31*, 64–71.
- (2) Howard, J. B.; Rees, D. C. *Chem. Rev.* **1996**, *96*, 2965–2982.
- (3) Burgess, B. K.; Lowe, D. J. *Chem. Rev.* **1996**, *96*, 2983–3011.
- (4) Rees, D. C.; Howard, J. B. *Curr. Opin. Chem. Biol.* **2000**, *4*, 559–566.
- (5) Howard, J. B.; Rees, D. C. *Proc. Natl. Acad. Sci. U.S.A.* **2006**, *103*, 17088–93.
- (6) Hoffman, B. M.; Dean, D. R.; Seefeldt, L. C. *Acc. Chem. Res.* **2009**, *42*, 609–19.
- (7) Thorneley, R. N.; Lowe, D. J. *Biochem. J.* **1983**, *215*, 393–403.
- (8) Danyal, K.; Inglet, B. S.; Vincent, K. A.; Barney, B. M.; Hoffman, B. M.; Armstrong, F. A.; Dean, D. R.; Seefeldt, L. C. *J. Am. Chem. Soc.* **2010**, *132*, 13197–9.
- (9) Roth, L. E.; Nguyen, J. C.; Tezcan, F. A. *J. Am. Chem. Soc.* **2010**, *132*, 13672–4.
- (10) Roth, L. E.; Tezcan, F. A. *ChemCatChem* **2011**, *3*, 1549–1555.
- (11) Nonbiological, light-driven platforms have been used to catalyze 6- or even 8-electron reduction reactions. See, for example: Morris, A. J.; Meyer, G. J.; Fujita, E. *Acc. Chem. Res.* **2009**, *42*, 1983. Cole, E. B.; Bocarsly, A. B. In *Carbon Dioxide as Chemical Feed-stock*; Aresta, M., Ed.; Wiley-VCH: Weinheim, Germany, 2010; p 291; Collin, J. P.; Sauvage, J. P. *Coord. Chem. Rev.* **1989**, *93*, 245.
- (12) Lee, C. C.; Hu, Y. L.; Ribbe, M. W. *Science* **2010**, *329*, 642–642.
- (13) Hu, Y.; Lee, C. C.; Ribbe, M. W. *Science* **2011**, *333*, 753–5.
- (14) Seefeldt, L. C.; Rasche, M. E.; Ensign, S. A. *Biochemistry* **1995**, *34*, 5382–5389.
- (15) Hardy, R. W.; Knight, E., Jr. *Biochim. Biophys. Acta* **1967**, *139*, 69–90.
- (16) Lowe, D. J.; Fisher, K.; Thorneley, R. N.; Vaughn, S. A.; Burgess, B. K. *Biochemistry* **1989**, *28*, 8460–6.
- (17) Li, J.; Burgess, B. K.; Corbin, J. L. *Biochemistry* **1982**, *21*, 4393–402.
- (18) Fisher, K.; Dilworth, M. J.; Newton, W. E. *Biochemistry* **2006**, *45*, 4190–8.
- (19) Lee, C. C.; Hu, Y. L.; Ribbe, M. W. *Angew. Chem., Int. Ed.* **2012**, *51*, 1947–1949.
- (20) Thorneley, R. N.; Lowe, D. J. Kinetics and mechanism of the nitrogenase enzyme. In *Molybdenum Enzymes*; Wiley-Interscience Publications: Hoboken, NJ, 1985; pp 221–284.
- (21) Castellano, F. N.; Dattelbaum, J. D.; Lakowicz, J. R. *Anal. Biochem.* **1998**, *255*, 165–70.
- (22) Corbin, J. L. *Appl. Environ. Microbiol.* **1984**, *47*, 1027–30.
- (23) Danyal, K.; Mayweather, D.; Dean, D. R.; Seefeldt, L. C.; Hoffman, B. M. *J. Am. Chem. Soc.* **2010**, *132*, 6894–6895.
- (24) Pham, D. N.; Burgess, B. K. *Biochemistry* **1993**, *32*, 13725–31.